NANO LETTERS

Letter

Low-Temperature Nanocrystal Unification through Rotations and Relaxations Probed by in Situ Transmission Electron Microscopy

Marijn A. van Huis, Lucas T. Kunneman, Karin Overgaag, Qiang Xu,
Gregory Pandraud, Henny W. Zandbergen, and Danie#l Vanmaekelbergh

Nano Lett., **2008**, 8 (11), 3959-3963 • DOI: 10.1021/nl8024467 • Publication Date (Web): 25 September 2008

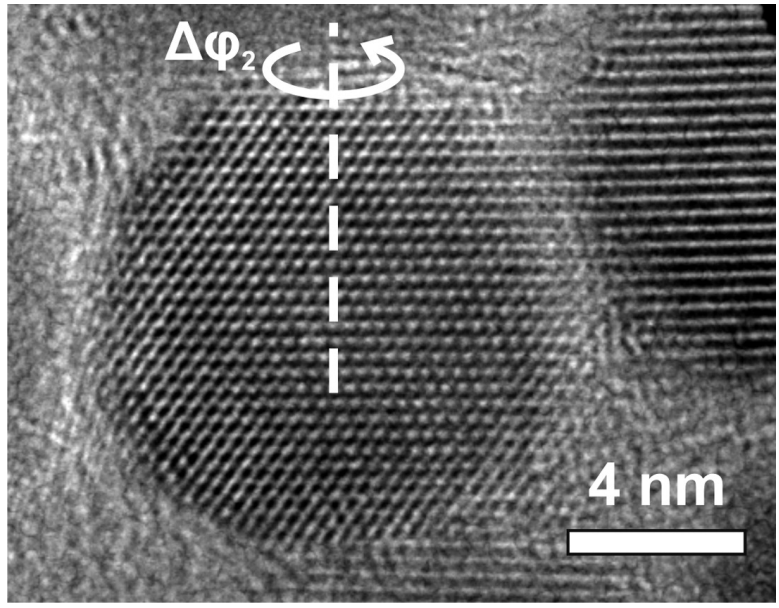

More About This Article

Additional resources and features associated with this article are available within the HTML version:

- Supporting Information
- Access to high resolution figures
- Links to articles and content related to this article
- Copyright permission to reproduce figures and/or text from this article

View the Full Text HTML

NANO LETTERS

2008
Vol. 8, No. 11
3959-3963

Low-Temperature Nanocrystal Unification through Rotations and Relaxations Probed by in Situ Transmission Electron Microscopy

Marijn A. van Huis,*,† Lucas T. Kunneman,‡ Karin Overgaag,‡ Qiang Xu,† Gregory Pandraud,† Henny W. Zandbergen,† and Daniël Vanmaekelbergh‡

Kavli Institute of Nanoscience, Delft University of Technology, Lorentzweg 1, 2628 CJ Delft, The Netherlands, and Condensed Matter and Interfaces, Debije Institute, Utrecht University, Princetonplein 1, 3508 TH Utrecht, The Netherlands

Received August 12, 2008; Revised Manuscript Received September 11, 2008

ABSTRACT

Through the mechanism of "oriented attachment", small nanocrystals can fuse into a wide variety of one- and two-dimensional nanostructures. This fusion phenomenon is investigated in detail by low-temperature annealing of a two-dimensional array of 10 nm-sized PbSe nanocrystals, in situ in the transmission electron microscope. We have revealed a complex chain of processes; after coalescence, the connected nanocrystals undergo consecutive rotations in three-dimensional space, followed by drastic interfacial relaxations whereby full fusion is obtained.

The low-temperature fusion mechanism of nanoclusters, which is driven mainly by reduction of surface energy, is inherently very complex since it requires three-dimensional (3D) reorientations of the nanocrystals and removal of interfaces. This so-called "oriented attachment" enables the formation of larger crystals with a wide variety of morphologies.[1−5] These processes typically take place far below the melting temperature of the bulk material. Understanding the fusion mechanism is of importance both to prevent degradation of nanocrystal superlattices and to control the formation of one- (1D) and two- (2D) dimensional nanostructures by fusion of smaller nanocrystal units. More generally, the mechanism provides a new perspective on the complex process of sintering of nanocrystalline materials, a method extensively used in materials science and industry.[6]

Due to systematic progress in wet chemical synthesis, many types of colloidal nanocrystals of metal and semiconductor compounds can be currently obtained with increasing control over the surface chemistry, size, and shape.[3,7] Colloidal crystallization from nanocrystal suspensions has led to nanocrystal superlattices with an astounding long-range order and a remarkable variation in the structure and stoichiometry.[8−10] Such superlattices may form the basis for new materials with collective properties that arise from quantum mechanical and dielectric interactions between the nanocrystal building blocks.[11−14] The separation of the monolayer-protected nanocrystals is a critical point that has become apparent by neck-formation between monolayer-protected gold nanocrystals in a Au superlattice.[15] Understanding the fusion mechanism and its energetics is thus required to ascertain long-term stability of superlattices.

In other applications, beneficial use is made of the tendency of nanocrystals to fuse, such as in the fabrication of larger single-crystals with 1D and 2D geometries. Manufacturing of opto-electronic components could be based on the cost-effective nanocrystal processing from a solution and subsequent thermal treatment. That nanocrystal fusion is a realistic option is supported by many reports in the field of colloidal nanoscience.[1,3,7,16] PbSe nanostructures can be formed from smaller nanocrystal building blocks through the process of oriented attachment.[2,4,5,17,18] These examples show the huge potential of spontaneous nanocrystal fusion for materials science. In addition, sintering and gentle annealing of polycrystalline materials is extensively used in the industry to improve the performance of materials.[6] Exact knowledge of the nanoscopic processes is often lacking; it can however be expected that processes take place similar to those observed with colloidal nanocrystals.

Here, we present a real time microscopic study of the entire chain of processes involved in the unification of PbSe nanocrystals into larger single crystals at temperatures far below the PbSe melting temperature[19] of 1079 °C. In order to obtain high resolution at elevated temperature, an advanced

* To whom correspondence should be addressed. E-mail: m.a.vanhuis@tudelft.nl. Tel: +31 15 2782272. Fax: +31 15 2786600.
† Delft University of Technology.
‡ Utrecht University.

10.1021/nl8024467 CCC: $40.75
Published on Web 09/25/2008

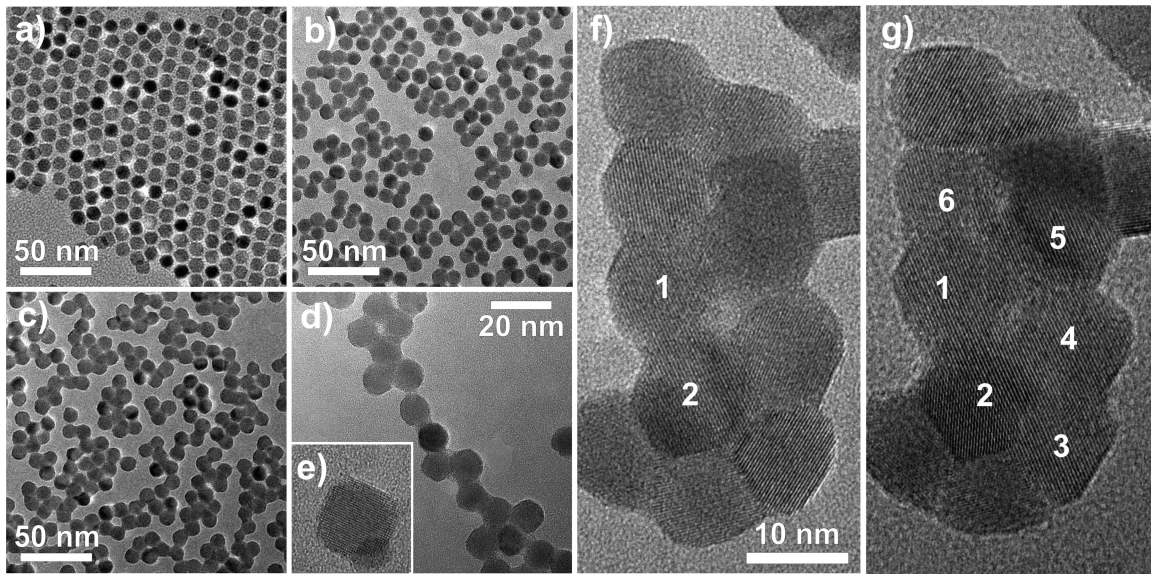

Figure 1. TEM images displaying the attachment and fusion process of PbSe quantum dots (QDs). (a) Starting configuration: two-dimensional array of 10 nm sized PbSe nanoclusters on a SiN substrate. The array shows hexagonal ordering. (b,c) Upon gentle annealing at a temperature of 100 °C, the QDs become mobile. Coalescence and initial attachment takes place. (d) In low-density areas, strings of QDs are formed. (e) Isolated QDs tend to adopt a truncated cubic morphology. (f,g) Continued annealing at 130 and 150 °C leads to crystal unification. (f) Agglomeration of some 11 connected QDs. Dots no. 1 and no. 2 have fused into a two-dot single crystal. (g) The same agglomeration 10 min later. Dots nos. 3−6 have fused with dots nos. 1−2 into a six-dot single crystal.

SiN heating chip[20] enabling low-drift transmission electron microscopy (TEM) imaging was used as a substrate for the quantum dots. Details on the in situ TEM heating are in the Supporting Information. In our study, we have used PbSe nanocrystals of 9.8 ± 0.5 nm in diameter where the original oleic acid capping is replaced by hexylamine capping.[18] Two-dimensional arrays of hexylamine-capped PbSe nanocrystals were prepared by drop-casting suspensions in toluene on the SiN chip and solvent evaporation. In general, attachment and fusion of the hexylamine-capped PbSe quantum dots occurred more easily (faster and at lower temperature) than when samples consisting of oleic acid-capped nanocrystals were used. Arrays based on smaller PbSe nanocrystals led to the same results as will be presented below. For TEM imaging, a Tecnai TF20-ST microscope operating at 200 kV was used, and a CM300-UT microscope operating at 300 kV and equipped with a fast-scan Tietz camera.

Figure 1 shows the main stages of single-crystal formation from an array of 10-nm sized PbSe nanocrystals. Figure 1a shows the initial configuration, an hexagonally ordered, two-dimensional array of PbSe quantum dots (QDs), with all dots separated by the hexylamine capping. In situ heating of this ordered array to 100 °C (Figure 1b,c) leads to a transition during which the nanocrystals have high mobility. The array becomes increasingly disordered, the nanoparticles coalesce, and initial attachment takes place. In low-coverage areas, 1D strings of QDs are formed as shown in Figure 1d, while isolated dots tend to adopt a cubic morphology (Figure 1e) in agreement with reports in the literature.[4] Larger, two-dimensional agglomerations are formed during annealing at 130 °C as shown in Figure 1f. Polynanocrystals are formed whereby the original dots can still be distinguished as individual nanocrystals. Within a time scale of minutes, these dots then fuse into multidot single crystals. Figure 1f shows

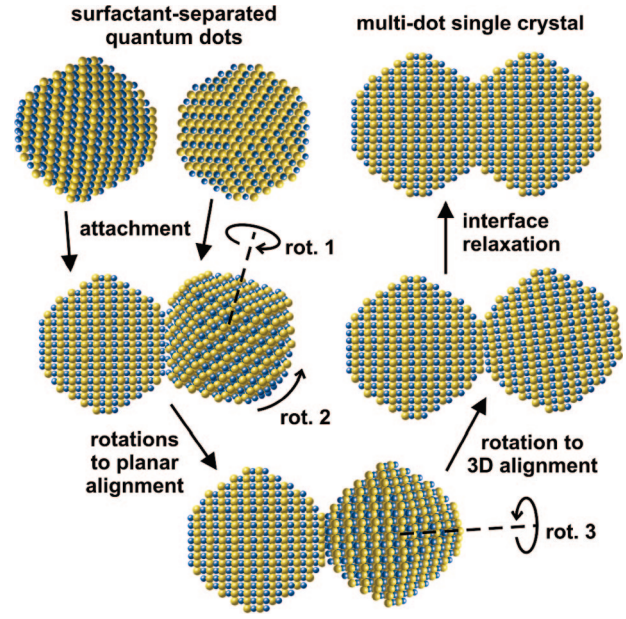

Figure 2. Schematic representation of the entire fusion process: (i) attachment due to surfactant evaporation, (ii) rotations to a planar alignment, (iii) subsequent rotation to a nearly full 3D alignment, and (iv) relaxations resulting in removal of the defective interface in order to achieve complete fusion. Experimental observations of rotations are displayed in Figures 3 and 4, interface relaxation is shown in Figure 4.

an agglomeration of eleven nanodots at 130 °C, including two dots (no. 1 and no. 2) that have already fused. Upon continued annealing for 10 min at a temperature of 150 °C, four other dots (nos. 3−6) have fused with the two-dot crystal so that a six-dot single crystal is formed in Figure 1g. Because the fusion is achieved without melting, the nanocrystals have to rotate over large angles and interfaces have

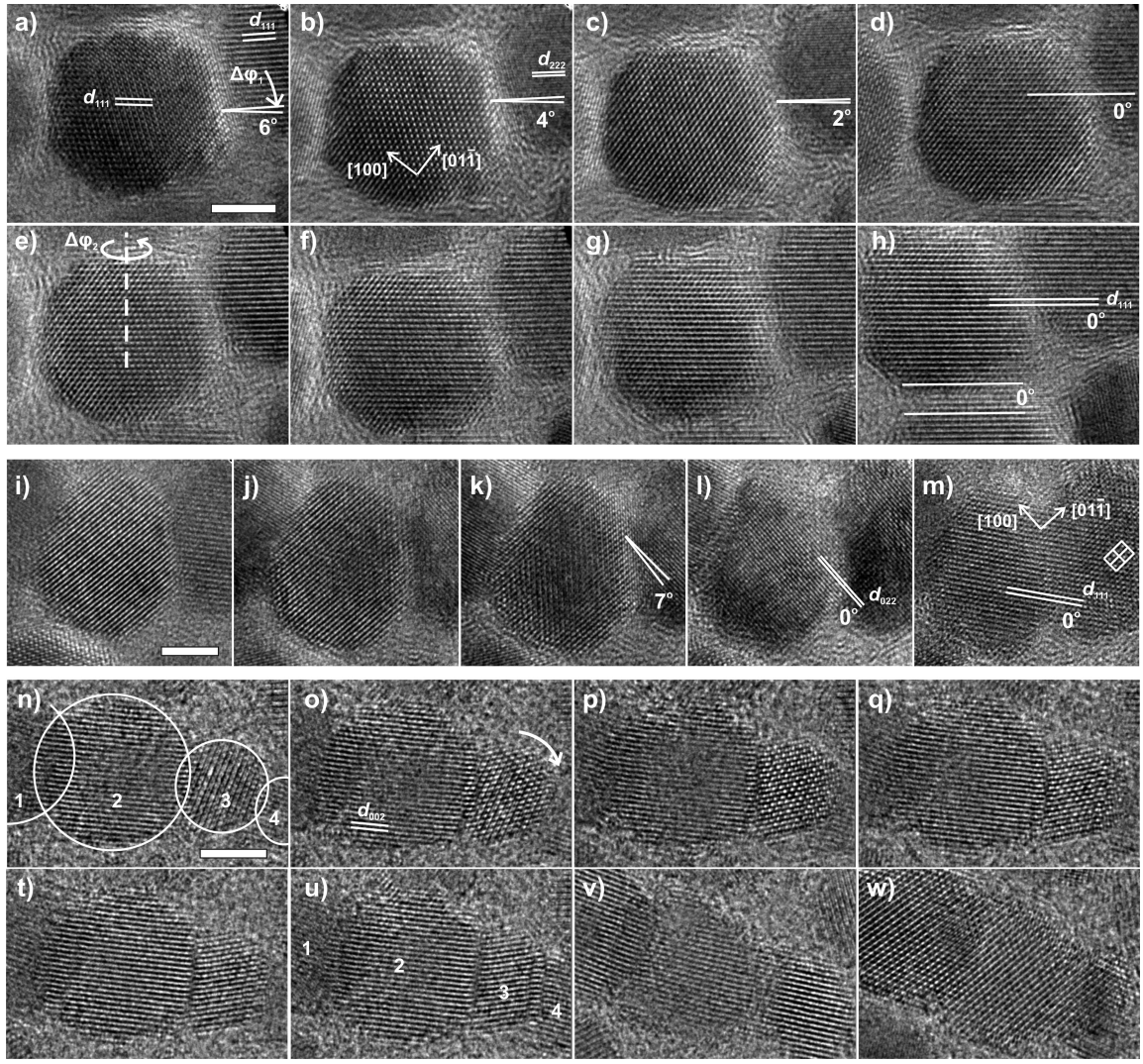

Figure 3. Stills of in situ TEM recordings, showing the evolution PbSe quantum dots (QDs) during three fusion events. The scale bars indicate 4 nm. In general, one QD is centered in the field of view because it is not known beforehand with which other QD it will fuse. (a−h) First event, two 10 nm PbSe QDs fuse into a single crystal at a temperature of 120 °C. Panels a−d: Rotation over 6° in the plane of view, establishing alignment of the (111) planes in panels d and e. Panels e−h: Subsequent rotation of the central nanocluster perpendicular to the field of view. A third QD attaches at the bottom in image h. (i−m) Second event, two 10 nm QDs with hexylamine capping fusing at a temperature of 120 °C. Panels k and l: A rotation of 7° removes the misalignment between the (022) planes, 3D alignment is obtained in panel m where the fused crystal is projected along (011). (n−w) Multisized PbSe QDs fusing into a nanorod. Panels n−u: The small nanocluster no. 3 rotates to align with the larger dot at its left. Movie 3 in the Supporting Information shows that the rotation is not smooth, but irregular as a function of time. Panel v: Four dots have fused into a 4 dot single crystal. The small dot that rotated has been assimilated into the rod. Panel w: The rod has rotated around its own axis, changing the projection of the crystal.

to be resolved. Note that all of this happens far below the melting temperature of PbSe (1079 °C).

Figure 2 shows schematically the mechanism of attachment and crystal unification, which was built from the TEM observations. First, the quantum dots attach after removal of the capping, whereby an interface is formed at the neck between the dots. Second, the quantum dots undergo several rotations, leading to partial alignment of the two nanocrystals. Here alignment of the (111) lattice planes is shown, which is known to be a preferential contact plane in specific chemical environments because of dipole interactions[4,17] (PbSe has the rocksalt crystal structure with a lattice parameter of 0.613 nm, and the {111} surfaces are electrically charged, Pb- or Se-terminated planes). While the (111) planes are aligned, the two crystals may still be rotated with respect to each other inside that plane. Hence, there is only planar alignment and another rotation is required leading to a nearly full alignment of the nanocrystals (3D alignment). In general, defects are still present at the interface between the two nanocrystals.[21,22] The last step toward complete fusion consists of atomic reconfigurations at the interface whereby these defects are removed. Note that not all rotations are equivalent: rotations 1 and 2 in Figure 2 will have the tendency to "tear open" the interface at one side and to compress it at the other side. Rotation 3 however, rotation perpendicular to the interface, involves only sliding of lattice planes over each other. The rotations can happen in different order and partially simultaneously. From a mathematical point of view, each fusion process is a particular path in the five-parameter space, a model which is often used to describe

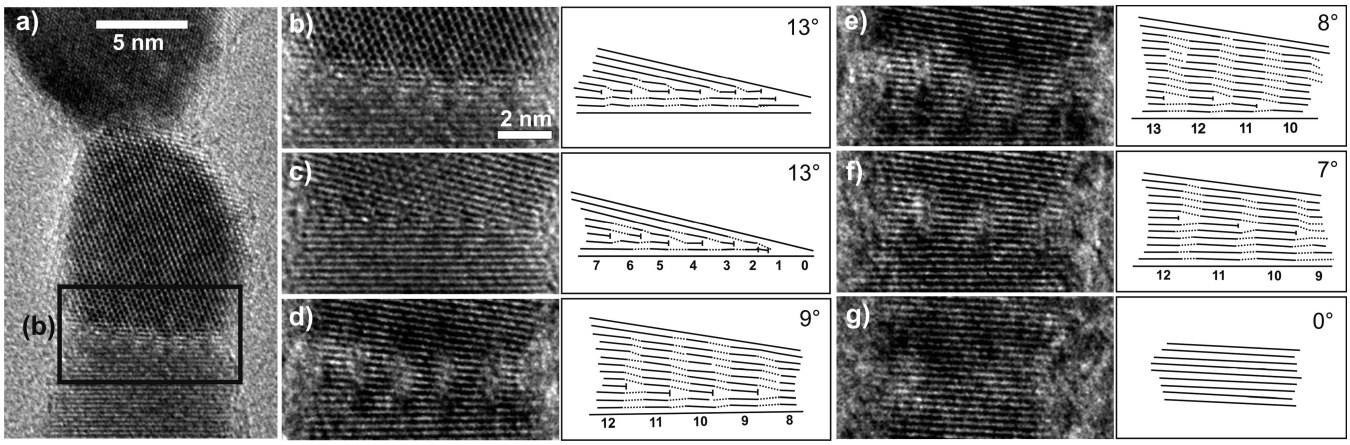

Figure 4. Rotations followed by interface relaxation, imaged during heating of 10 nm sized PbSe QDs at a temperature of 170 °C, increasing to 200 °C, over a time span of 23 min. (a) Triplet of attached quantum dots with interfaces. The two dots at the bottom fuse into a single crystal. (b−g) Details of the bottom interface. Lattice planes drawn from the images are shown on the right-hand side. (b) The dots are not aligned. (c) The top QD has rotated, so that both crystals now display the same line pattern with a mistilt of φ=13°. The interface is very sharp and involves only a few atomic layers, in which 7 interface dislocations can be identified (displayed schematically on the right-hand side of the image). (d) The mistilt has decreased to $\varphi = 9°$ through a reduction of the number of interface dislocations to 4. Also the interface area broadens as the dislocations evolve and produce strain fields also in atomic layers further away from the interface. (e,f) Further decrease of the mistilt to 8 and 7° accompanied by a decrease of the number of dislocations. (g) There are no dislocations left; the crystals have fused into a single crystal.

the grain boundary character distribution in a volume of polycrystalline material.[23,24] Here three parameters are required to specify the misalignment of the two crystals, while two parameters are required to specify the orientation of the interface.

Figure 3 shows three events of fusing nanoclusters, recorded real-time, in situ in the electron microscope. Movies 1, 2, and 3 in the Supporting Information show a selection of the rotational movements of these events. In general, the two fusing nanoclusters both undergo rotations. They interact with each other but also with the other surrounding nanoclusters through multiple, competing attachments. In general, planar alignment precedes the 3D alignment of the crystals. Figure 3a−d shows an event in which a mistilt between (111) lattice planes of 6° decreases gradually to 4, 2, and 0° (±0.5°), so that planar alignment is achieved in Figure 3d,e. Here the lattice planes extend horizontally over the two nanoclusters, while from the different image contrast (dots for the central PbSe cluster and lines for the cluster on the right) it is clear that the crystal orientation of the two dots is not the same. In Figure 3h, a few minutes later both nanoclusters display the same contrast, which proves that the central cluster has rotated and which suggests 3D alignment.

In the next event shown in Figure 3i−m, the crystals do not seem aligned at all at first, then they rotate so that a misalignment of the (022) planes of 7° is reduced to 0° (Figure 3k,l), which is followed by a full 3D alignment in Figure 3m, where both crystals now show the same 2D contrast. The identifiable (011) projection of the two crystals is a proof of 3D alignment. Also in other recorded series, subsequent rotations are observed (Figure 3o to 3t to 3v, and Figure 4b to 4c to 4g). In particular in Supporting Information Movie 3 (corresponding to Figure 3n−u), it is clear that the rotation is not a smooth, continuous movement. The small nanocluster no. 3 is rotating with irregular angular velocity into the right position in order to align with the larger nanocluster no. 2 at its left. Furthermore, the QDs seem to partially overlap in projection (overlapping circles), which means that the interfaces are not parallel with the electron beam. Probably the crystallographic interactions between the dots are much stronger than the adhesion to the SiN substrate, so that an approximate zigzag chain is formed whereby some dots are positioned higher with respect to the substrate than others (e.g., a side projection of the PbSe line in Figure 1d would also show projections of interfaces). Eventually, the four dots fuse into a single crystal nanorod in Figure 3w.

The last step in the fusion process consists of interface relaxation, which is displayed in Figure 4. First the PbSe nanocrystal at the top side of the interface rotates to achieve planar alignment (Figure 4b to Figure 4c), after which a mistilt of $\varphi = 13°$ is observed between the two crystals in the plane of the image.

The atomic planes stop quite abruptly at the interface, and therefore the interface consists of only a few atomic layers. Seven edge dislocations (partial lattice planes) can be distinguished, equally distributed along the interface.[21,22] When the mistilt becomes smaller (9° in Figure 4d), the edge dislocations induce strain fields[25] extending into the lattices away from the interface. At this point, the rotation becomes more difficult because the well-developed dislocations are lowering the interface energy. Every time that an edge dislocation is removed, the mistilt decreases in a stepwise manner from $\varphi = 13$ to 9, 8, 7° (Figures 4c−f), until no dislocations are left, the interface has disappeared ($\varphi = 0°$), and the fusion is completed (Figure 4g). Although this particular observation clarifies the process of interface relaxation, in general the last step of the fusion process seemed to happen much faster (in a few minutes) than in this particular case (23 min). Probably the fusion process

happens more easily when the interfaces at the necks between the dots are still small, and when the rotational misalignment of the two nanocrystals is small at the moment of first attachment.

Summarizing, gentle annealing at a temperature of 100 °C first induces removal of the capping of the spherical PbSe quantum dots, enabling attachment and interface formation at the necks between the dots. Second, rotations establish a planar alignment of the two nanocrystals, followed by another rotation step establishing near-3D alignment with interfacial defects. Finally, the interface is removed as remaining edge dislocations disappear one by one. The results suggest a weak interaction between the nanocrystals and the amorphous SiN support. It is astonishing that the nanocrystals can rotate seemingly easily (in a time scale of seconds) while the interfaces remain in place. This is only possible when massive atomic reconfigurations generate continuous interface relaxation. Undoubtedly, during these rotations the interface will be strongly disordered in the first few atomic planes. All these rotations and interfacial reconfigurations occur at temperatures much lower than the melting temperature of bulk PbSe.

The fusion is driven by a reduction of the surface and interfacial energy that forms a considerable fraction of the total free energy of the system. Given the fact that thermal motion of the nanocrystals must be random (noninteracting, spatially separated nanocrystals can also undergo thermally induced rotations[26]), it is striking that the complex process seems to be directed toward crystal fusion. The removal of the capping molecules increases the surface energy of the nanocrystals considerably, and therefore coalescence resulting in a reduction of the surface energy is favored. Interaction between nanocrystal dipoles, caused by charged {111} facets, can induce preferential oriented attachment and string formation,[4,5,17] although the contribution of these interactions to the total free energy is difficult to quantify. Understanding the second step in the process of fusion, that is, the consecutive rotations leading to nanocrystal alignment, will need detailed microscopic simulations. The last step, the removal of the misfit in the interface, must be driven by a reduction of the interfacial energy. Our observations shed a first light on this intriguing process that occurs at low temperature without observable melting. Atomistic simulation studies of the evolution of the free energy of the system during the distinct steps toward fusion will be required for a full understanding.

Acknowledgment. The authors acknowledge financial support from the Stichting Technologie en Wetenschap (STW, Project No. 07532), the Stichting Fundamenteel Onderzoek der Materie (FOM), The Netherlands, and from the European Union Framework 6 program, ref. 026019 ESTEEM.

Supporting Information Available: Details on the in situ TEM heating are given. Furthermore, three real-time, in situ TEM movies are included showing a selection of the three-dimensional rotations displayed in Figure 3. This material is available free of charge via the Internet at http://pubs.acs.org.

References

(1) Tang, Z.; Kotov, N. A.; Giersig, M. *Science* **2002**, *297*, 237–240.
(2) Lifshitz, E.; Bashouti, M.; Kloper, V.; Kigel, A.; Eisen, M. S.; Berger, S. *Nano Lett.* **2003**, *3*, 857–862.
(3) Yin, Y.; Alivisatos, A. P. *Nature* **2005**, *437*, 664–670.
(4) Cho, K.-S.; Talapin, D. V.; Gaschler, W.; Murray, C. B. *J. Am. Chem. Soc.* **2005**, *127*, 7140–7147.
(5) Klokkenburg, M.; Houtepen, A. J.; Koole, R.; de Folter, J. W. J.; Erné, B. H.; van Faassen, E.; Vanmaekelbergh, D. *Nano Lett.* **2007**, *7*, 2931–2936.
(6) Lu, K. *Int. Mater. Rev.* **2008**, *53*, 21–38.
(7) Min, Y.; Akbulut, M.; Kristiansen, K.; Golan, Y.; Israelachvili, J. *Nat. Mater.* **2008**, *7*, 527–538.
(8) Murray, C. B.; Kagan, C. R.; Bawendi, M. G. *Science* **1995**, *270*, 1335–1338.
(9) Redl, F. X.; Cho, K.-S.; Murray, C. B.; O'Brien, S. *Nature* **2003**, *423*, 968–971.
(10) Shevchenko, E. V.; Talapin, D. V.; Kotov, N. A.; O'Brien, S.; Murray, C. B. *Nature* **2006**, *439*, 55–59.
(11) Talapin, D. V.; Murray, C. B. *Science* **2005**, *310*, 86–89.
(12) Vanmaekelbergh, D.; Liljeroth, P. *Chem. Soc. Rev.* **2005**, *34*, 299–312.
(13) Liljeroth, P.; Overgaag, K.; Urbieta, A.; Grandidier, B.; Hickey, S. G.; Vanmaekelbergh, D. *Phys. Rev. Lett.* **2006**, *97*, 096803.
(14) Luther, J. M.; Beard, M. C.; Song, Q.; Law, M.; Ellingson, R. J.; Nozik, A. J. *Nano Lett.* **2007**, *7*, 1779–1784.
(15) Kiely, C. J.; Fink, J.; Brust, M.; Bethell, D.; Schiffrin, D. J. *Nature* **1998**, *396*, 444–446.
(16) Courty, A.; Henry, A.-I.; Goubet, N.; Pileni, M.-P. *Nat. Mater.* **2007**, *6*, 900–907.
(17) Talapin, D. V.; Black, C. T.; Kagan, C. R.; Shevchenko, E. V.; Afzali, A.; Murray, C. B. *J. Phys. Chem. C* **2007**, *111*, 13244–13249.
(18) Houtepen, A. J.; Koole, R.; Vanmaekelbergh, D.; Meeldijk, J.; Hickey, S. G. *J. Am. Chem. Soc.* **2006**, *128*, 6792–6793.
(19) Lin, J. C.; Sharma, R. C.; Chang, Y. A. *J. Phase Equilib. Diffus.* **1996**, *17*, 253–260.
(20) Creemer, J. F.; Helveg, S.; Hoveling, G. H.; Ullmann, S.; Molenbroek, A. M.; Sarro, P. M.; Zandbergen, H. W. *Ultramicroscopy* **2008**, *108*, 993–998.
(21) Penn, R. L.; Banfield, J. F. *Science* **1998**, *281*, 969–971.
(22) Tsai, M. H.; Chen, S. Y.; Shen, P. *Nano Lett.* **2004**, *4*, 1197–1201.
(23) Saylor, D. M.; Morawiec, A.; Rohrer, G. S. *Acta Mater.* **2003**, *51*, 3675–3686.
(24) Rohrer, G. S.; Randle, V.; Kim, C.-S.; Hu, Y. *Acta Mater.* **2006**, *54*, 4489–4502.
(25) It is unlikely that these large fringes are caused by rotational Moiré, because the interface is quite sharp in Figure 4c.
(26) Be'er, A.; Kofman, R.; Phillipp, F.; Lereah, Y. *Phys. Rev. B* **2007**, *76*, 075410.

NL8024467